

# Calibrating Human Hand for Teleoperating the HIT/DLR Hand

Haiying Hu, Xiaohui Gao, Jiawei Li, Jie Wang

Robot Research Institute  
Harbin Institute of Technology (HIT)  
150001 Harbin, P.R. China  
huhaiying@hit.edu.cn

Hong Liu

Institute of Robotics and Mechatronics  
German Aerospace Center, DLR  
82230 Wessling, Germany  
hong.liu@dlr.de

**Abstract** - Using human action to guide robot execution can greatly reduce the planning complexity. We calibrate a human hand model and map its motion to a four-finger dexterous robot hand. The parameters of human hand model are determined by open-loop kinematic calibration method based a vision system. We analyze the kinematic difference between the human hand and dexterous robot hand, and present a modified fingertip mapping to solve the partial overlap of the fingertip workspaces. 3D graphic simulation and manipulation experiments show that the accuracy of the human hand model and the mapping method are sufficiently precise for teleoperation tasks.

**Index Terms** - human hand model; dexterous robot hand; open-loop calibration; mapping; teleoperation

## I. INTRODUCTION

The human hand is a powerful and complex device for teleoperating dexterous robot hand. As the teleoperation tasks become more delicate and difficult, the accuracy of the human hand model is required to achieve. The goal of our research is to provide an interface with a dataglove that enable people possibly easily and precisely teleoperate the HIT/DLR four-finger dexterous hand, as shown in Fig.1. The main difficulties arise from two aspects: calibrating the human hand model for obtaining the precise position and orientation of the fingers; mapping the human hand motion to the robot hand.

In recent years, many researchers have devoted their attention to such problems. Because of the very complex structure of the human hand, a number of simplifications must incorporate into a tractable hand model for calibrating a particular human hand. The open-loop calibration technique described in this paper was applied to identify kinematic parameters of the index finger with the Utah Dexterous Hand Master [1], which had an accuracy of about 2 mm. Without developing a human hand model, Fischer [2] directly tracked the fingertips positions based a vision system. By using a neural network, they achieved tip position errors less than 1.8 mm. The closed-loop kinematic calibration method was applied to calibrate the human hand model [3], which was called “zero-hardware solution” requiring touching each fingertip to thumb during the calibration procedure.

The kinematic workspaces of human hand and robot hand are generally different; people still want to make the mapping intuitively to the teleoperator. In [4], by limiting the allowable motions of the human hand, the motion mapping to the robot hand was simplified. In [5], An optimized fingertip mapping

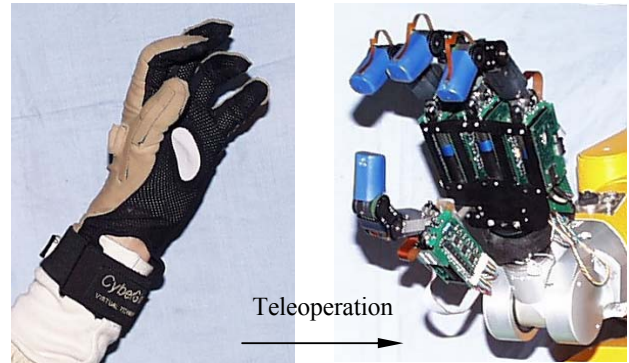


Fig.1: HIT/DLR dexterous robot hand teleoperation by a dataglove

methods generated robot hand poses by prioritizing the human fingertip position, orientation and minimizing the errors.

In the following sections, we first describe the overall calibration system simply, and then present a kinematic model of human hand and an open-loop calibration routine based a vision system, which can quickly and accurately identify the parameters of human hand model. In the next section, we transform the motions of an unconstrained human hand to the HIT/DLR dexterous robot hand by the modified fingertip mapping. Then we test the calibration and the mapping method in a simulation system and a teleoperation system with vision and force feedback. Finally, we address the conclusion and future work.

## II. OVERALL CALIBRATION SYSTEM DESCRIPTION

The calibration routine proceeds as following: An operator wears the dataglove and moves fingers freely while the wrist is fixed on the table. The vision system captures a series of 'poses' of fingers and measures the exact fingertip positions of each finger. At the same time, the uncalibrated raw sensor values of the dataglove are also recorded. Based on the kinematic knowledge of the hand model, we can come up with an iterative solution minimizing the errors between the calculated fingertip positions and the measured fingertip positions by the vision system. After several iterations, we can obtain stable and actual parameters' values of the human hand model, so we can calculate the fingertip positions of the operator in real time, which only with the sensor readings from the dataglove.

### A. CyberGlove® and Vision System



Fig.2: CyberGlove® and vision system

As shown in Fig. 2, we use CyberGlove® as a left hand input device, which is constructed with stretch fabric and 23 resistive bend sensors that describe the five fingers' joint angles and the orientation of the hand. Fig. 3 shows the joint sensors' locations at the human hand model. Although CyberGlove® is shipped with calibration software, the fingertip positions obtained this way are not precise enough to control a dexterous robot hand.

In order to measure the fingertip positions of human fingers with the vision system, we marked each fingertip of the dataglove with a coloured sticker (LED). We used two calibrated stereo camera to capture the four coloured stickers in real time, from which the 3D positions of the coloured markers were computed using a Datacube MaxPCI board. The computer recorded 60 distinct fingertip positions (in the  $x$ ,  $y$ ,  $z$  direction) for each finger and the corresponding raw sensor data of the CyberGlove® for calibration.

### B. HIT/DLR Hand

Since 2001, based on the DLR's experience, HIT and DLR have developed a smaller human-like four-finger dexterous robot hand [6]. HIT/DLR hand is left dexterous hand, which is a multisensory and integrated four fingers with in total thirteen degrees of freedom (DOFs), which is approximately 1.5 times that of a human hand, as shown in Fig. 1. Each finger has three DOFs and four joints; last two joints are mechanically coupled by a rigid linkage (1DOF). The thumb has an additional DOF to realize the motion relative to the palm. This enables to use the hand in different configurations. In this hand, 13 commercial brushless DC motors with integrated analog Hall sensors systems as well as more than 100 sensors are integrated in the fingers and palm. DSP based control system is implemented in PCI bus architecture and the high speed serial communication between the hand and DSP needs only 3 cables. The high degree of integration and low weight (1.5kg for whole hand) make the HIT/DLR dexterous hand can be completely mounted on a robot arm.

## III. HUMAN HAND CALIBRATION

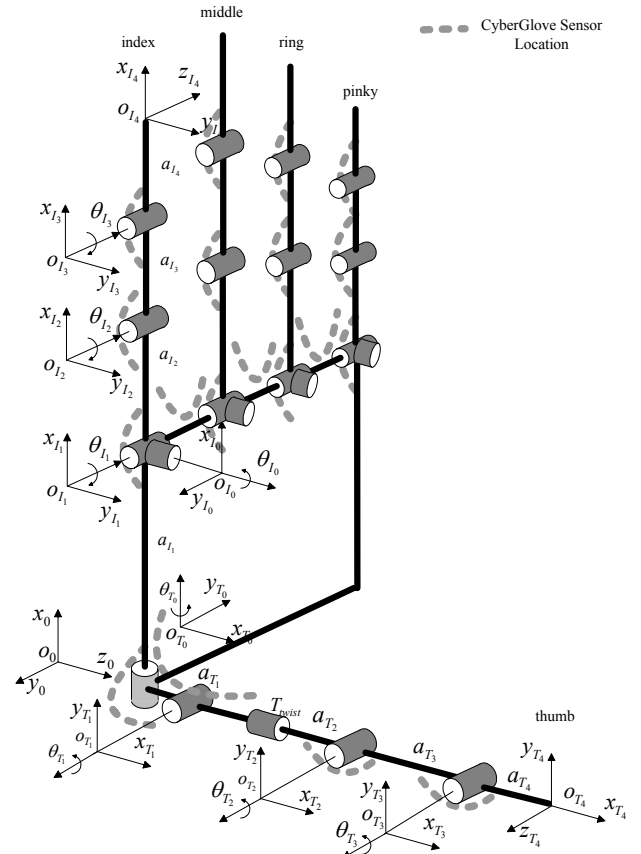


Fig.3: Human hand kinematic model and its D-H coordinate systems.

### A. Human Hand Model

In our case, we need a kinematic hand model that can possibly satisfy following three aspects by prioritizing:

- Accurately measuring and displaying human hand fingertip positions and poses.
- Finger joint configuration can finely match the joint sensor location of the CyberGlove®.
- Minimizing the kinematic differences with the HIT/DLR dexterous robot hand.

Our empirical examinations realized that the model developed by Rohling and Hollerbach [1], and Weston B.Griffin and Mark R. Cutkosky [3] can finely meet such requests. Fig. 3 shows a human left hand model. In the model, the human hand is converted to a mechanical linkage, with finger bones intersecting in Hookean pin joints. The model does not take into account effects such as soft tissue deformation or bone-on-bone sliding.

The base coordinate system ( $O_0$ ) for whole human hand is conveniently located at the point where the thumb and the index metacarpal meet. The metacarpal joint of thumb has two DOFs: The  $T_0$  joint is located at the base of the thumb with the axis of rotation along the index metacarpal. The  $T_1$  axis is offset from and orthogonal to the  $T_0$  axis. In order to account for the thumb pronation, an unsensed axis is placed along the

thumb metacarpal ( $T_{twist}$ ). The angle of  $T_{twist}$  joint is denoted as a linear function of the abduction ( $T_0$ ) and flexion ( $T_1$ ) [3]. The axis of rotation of the  $T_2$  and  $T_3$  are parallel.

The metacarpophalangeal joint of index finger has two orthogonal collocated DOFs: abduction ( $I_0$ ) and flexion ( $I_1$ ). The proximal interphalangeal joint ( $I_2$ ) and the distal interphalangeal joint ( $I_3$ ) are modeled as having one DOF. The axis of rotation of the  $I_1$ ,  $I_2$  and  $I_3$  are parallel. The other three fingers' kinematic models (middle, ring and pinky) are same with index finger. In the following calibration section, we mainly discuss the thumb and index finger.

Following traditional practice of modeling robot kinematics, a series of reference frames are selected for each of the finger joints. Robot kinematic transformations can be defined by Denavit-Hartenberg parameters. The transforms between each of the coordinate frames are described as:

$${}^{i-1}A_i = rot(z, \theta_i) trans(z, d_i) trans(x, a_i) rot(x, \alpha_i)$$

Where  $\theta_i$  is the joint angle,  $a_i$  is the length of link,  $\alpha_i$  is the twist angle,  $d_i$  is the offset length.

The fingertip position may be calculated if the fixed kinematic parameters are known and the variable ones are measured. The calculation can be done through homogeneous transforms. The fingertip positions of thumb respect to the  $O_0$  reference frame:

$${}^0d_{T4} = {}^0A_{T0} {}^{T0}A_{T1} {}^{T1}A_{T2} {}^{T2}A_{T3} {}^{T3}A_{T4} \quad (1)$$

The fingertip positions of the index finger respect to the  $O_0$  reference frame:

$${}^0d_{I4} = {}^0A_{I0} {}^{I0}A_{I1} {}^{I1}A_{I2} {}^{I2}A_{I3} {}^{I3}A_{I4} \quad (2)$$

### B. Hand Kinematic Parameters Need Calibration

The CyberGlove® measures human hand joint angles which can represent as following relation [7]:

$$\theta_i = g_i * \sigma_i + \beta_i \quad (3)$$

Where  $\sigma_i$  is the raw sensor value,  $g_i$  is the gain and  $\beta_i$  is the offset value. But some glove sensors are physically cross-coupled. For instance, the sensors located at the  $T_0$  and  $T_1$  joints are cross-coupled between the  $\theta_{T_0}$ ,  $\theta_{T_1}$ ,  $\theta_{Twist}$  angles of the model. Their relation can present as following matrix equation form:

$$\begin{bmatrix} \theta_{T_0} \\ \theta_{T_1} \\ \theta_{T_{twist}} \end{bmatrix} = \begin{bmatrix} g_{T_0} & g_{T_0}^{\sigma_1} \\ g_{T_1}^{\sigma_0} & g_{T_1} \\ g_{T_{twist}}^{\sigma_0} & g_{T_{twist}}^{\sigma_1} \end{bmatrix} \begin{bmatrix} \sigma_{T_0} \\ \sigma_{T_1} \end{bmatrix} + \begin{bmatrix} \beta_{T_0} \\ \beta_{T_1} \\ \beta_{T_{twist}} \end{bmatrix} \quad (4)$$

Note that the  $\theta_{Twist}$  parameter has no corresponding sensor value because the CyberGlove® does not measure this type of motion. The calibration software shipped with the CyberGlove® can give the preliminary value of each  $g_i$  and  $\beta_i$ . The initial length  $a_i$  can be measured for a typical user. In summary, our calibration optimized the parameters associated with the thumb are:

$$P_T = \begin{bmatrix} \beta_{T_0}, \beta_{T_1}, \beta_{T_{twist}}, \beta_{T_2}, \beta_{T_3}, a_{T_1}, a_{T_2}, a_{T_3}, a_{T_4}, \\ g_{T_0}, g_{T_1}, g_{T_2}, g_{T_3}, g_{T_0}^{\sigma_1}, g_{T_1}^{\sigma_0}, g_{T_{twist}}^{\sigma_0}, g_{T_{twist}}^{\sigma_1} \end{bmatrix}$$

The parameters needing calibration associated with the remaining three fingers are similar. For example, the parameters associated with the index finger are:

$$P_I = [\beta_{I_0}, \beta_{I_1}, \beta_{I_2}, \beta_{I_3}, a_{I_1}, a_{I_2}, a_{I_3}, a_{I_4}, g_{I_0}, g_{I_1}, g_{I_2}, g_{I_3}]$$

### C. Open-Loop Kinematic Calibration Method

To accurately determine human hand kinematic parameters, open loop kinematic calibration method [1] is used. The vision system is used to measure each fingertip positions. We can obtain the error vectors  $\Delta d$  between the fingertip positions measured by the vision system and the calculated ones by the human hand forward kinematics. After store  $m$  poses, we can yield an error vector of stacked endpoint position errors:

$$\begin{bmatrix} \Delta d_1 \\ \vdots \\ \Delta d_m \end{bmatrix} = \begin{bmatrix} C_1 \\ \vdots \\ C_m \end{bmatrix} \Delta \phi \quad (5)$$

Where  $\Delta d_p = [d_x \ d_y \ d_z]^T$ , error vector expressed in base frame ( $O_0$ ) at the pose  $p$ .  $C_p = [C_{\beta_1} \ \dots \ C_{a_i} \ \dots \ C_{g_i} \ \dots]$ , Jacobian matrix at pose  $p$  with respect to each kinematic parameter.  $\Delta \phi = [\Delta \beta_1 \ \dots \ \Delta a_i \ \dots \ \Delta g_i \ \dots]$ , variation vector of kinematic parameters.

Equation (5) can be expressed more compactly:

$$\Delta d = C \Delta \phi \quad (6)$$

Where Jacobian matrix  $C$  can easily be evaluated by screw vector analysis [8]:

$$[C_{\beta_i}] = [{}^0R] \{ \{ z_{i-1} \} \times \{ {}^{i-1}P_N \} \} \quad (7)$$

$$[C_{a_i}] = [{}_{i-1}^0 R] \{x_{i-1}\} \quad (8)$$

$$[C_{g_i}] = [C_{\beta_i}] \cdot \sigma_i \quad (9)$$

Where  $[ ]$ ,  $\{ \}$  and  $\times$  respectively denote matrix, vector and cross product;  $[{}_{i-1}^0 R]$  is the rotation matrix from frame  $(i-1)$  to the base frame  $(O_0)$ ;  $\{{}^{i-1}P_N\}$  is the finger tip position vector expressed in frame  $(i-1)$ ; and  $\{z_{i-1}\} = \{0,0,1\}^T$ ,  $\{x_{i-1}\} = \{1,0,0\}^T$ ,  $\sigma_i$  is the raw sensor value.

We can evaluate a least-squares solution of  $\Delta\phi$  based on singular value decomposition (SVD) of the Jacobian matrix  $C$ .

$$\Delta\phi = (C^T \cdot C)^{-1} \cdot C^T \cdot \Delta d \quad (10)$$

The parameters  $\phi$  are modified by  $\Delta\phi$  in an iterative process to minimize  $\Delta d$ . The iteration continues until parameters converge to stable value.

#### D. Parameters Scaling

In order to maintain acceptable variance of each parameter and get proper convergence in nonlinear optimization and for singular value decomposition, parameter scaling is implemented to improve the condition of identification problem by introducing a scaling matrix  $H = \text{diag}(h_1, \dots, h_r)$ . Schroer [9] proposes scaling based on the effect on the anticipated error of the robot (say 1 mm).

$$h_j(p) = \frac{10^{-3} m}{\| \text{column}(C_p) \|} \quad (11)$$

Where  $\text{column}(C_p)$  is extracted from Jacobian matrix  $C$  corresponding the parameter at the pose  $p$ , the scaling factor  $h_j(p)$  is defined as that parameter deviation that causes a 1 mm endpoint displacement. In order to make the pose set  $p$  sufficiently large and descriptive of all possible poses, then selecting  $h_j = \min h_j(p)$ . The most conservative estimate  $h_j$  over all poses is called the extremal scaling value. Then:

$$\Delta d = C \Delta\phi \rightarrow \Delta d = (CH)(H^{-1} \Delta\phi) \quad (12)$$

A low condition number  $k$  is required for good identifiably.

$$k = \|C\| \|C^{-1}\| = \sigma_1 / \sigma_r \quad (13)$$

Where  $C$  is the concatenated Jacobian matrix after scaling.  $C^{-1}$  is the pseudo-inverse of  $C$ ,  $\sigma_1$  is the largest singular value of  $C$ , and  $\sigma_r$  is the smallest value of  $C$ . Schroer suggested that the

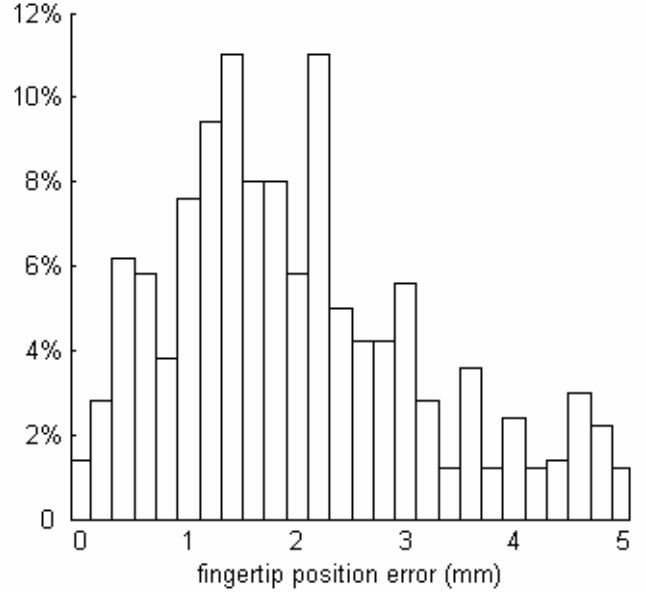


Fig.4 Distribution of fingertip position errors for 800 samples

condition number  $k$  should be less than 100. In our calibration procedure, each condition number  $k$  of the  $C$  matrix after scaling is less than 100.

#### E. Calibration Result

Calibration quality can be obtained by examining error vectors  $\Delta d(d_x, d_y, d_z)$  between the positions measured by the vision system and the calculated positions by the human hand forward kinematics with the calibrated parameters. We tested about 200 samples for each finger and all samples have errors less than 5mm. Fig. 4 shows the distribution of approximation fingertip position errors after calibration.

### IV. HUMAN TO ROBOT HAND FINGERTIP MAPPING

In general, there are two ways of mapping the human hand motion to robot hand: joint space mapping and Cartesian space mapping. The former is more suitable for enveloping (or power) grasps and the later is more suitable for fingertip (or precision) grasps [2]. After the calibration and knowing accurate joint angles of human hand fingers, the joint space mapping is easy to fulfill. We can directly transfer the calibrated joints value measured by the CyberGlove® to the robot hand. In the following, we present the fingertip position mapping in Cartesian space. The main problem is encountered similar to those discussed in previous research: human and robot hand kinematic dissimilarities result in a partial overlap of the fingertip workspaces.

#### A. Kinematic Difference Between Human and Robot Hand

- All four fingers of the HIT/DLR hand have the same structure and equal total finger length, which is about 1.5 times of the human hand. The motion range of each joint is the same. All base joint has two DOFs and the axis is perpendicular and intersected (abduction

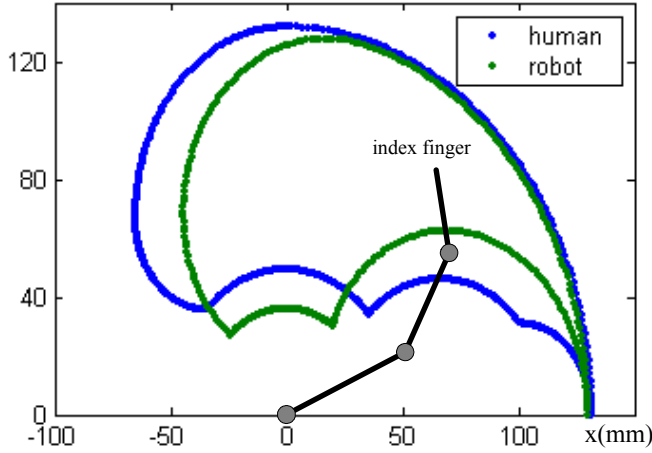


Fig.5 Workspace boundaries of human and robot index finger in a common reference frames when joint  $I_0=0$

$-20^\circ \sim 20^\circ$ , flexion  $-75^\circ \sim 75^\circ$ ), the last two joints are mechanically coupled ( $0^\circ \sim 90^\circ$ ).

- In our human hand, the total length of each finger is different and some joints motion ranges are different from the corresponding robot hand joint. For instance, the  $I_1$  joint of index finger has the motion range about  $0^\circ \sim 90^\circ$ . The thumb base joint has two DOFs:  $T_0$  (about  $0^\circ \sim 120^\circ$ ) and  $T_1$  (about  $30^\circ \sim 90^\circ$ ), the axis of  $T_1$  is perpendicular and offset from  $T_0$ . Especially, the thumb of human hand has an additional rotation freedom:  $T_{twist}$ .

In order to analysis and compare the workspace difference between human and robot hand, Fig. 5 shows the difference workspace boundaries for the index finger of HIT/DLR dexterous hand and the author's index finger in a plane where the joint  $I_0=0$ . Both fingers are shown in the common reference frame. The whole length of human index finger is linear scaled with a factor 1.5.

### B. Modified Fingertip Mapping

In order to manipulate the dexterous robot hand intuitively and easily, the workspace mapping should be only with a translation and a linear scaling with a constant factor in all DOFs. As shown in Fig. 5, some of the human hand fingertip positions after a linear scale are out of the dexterous robot hand workspace. When such situation happens, the approximate robot hand pose must be generated without introducing discontinuities between exact and approximate mapping. To solve the problem we developed the modified fingertip mapping method, which proceeds by following three steps:

- Calculating each fingertip positions of human hand by the forward kinematics with the calibrated parameters, which only need the raw reading dates of each joint from the CyberGlove®.
- Mapping each fingertip positions that are scaled with a linear factor to the robot hand via a common reference

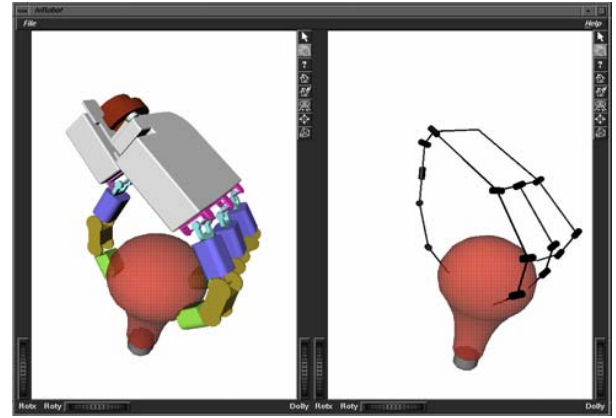


Fig.6 3D graphics simulation system for testing the modified fingertip mapping method. The left is the dexterous hand, the right is human hand.

frame. Calculating the inverse kinematics solutions of the dexterous robot hand.

- For where the fingertip positions are out of the dexterous robot hand workspace and the directly inverse kinematics solutions are not possible, approximate pose of the robot hand should be generated.

For instance, when the human thumb fingertip position is out of the dexterous robot hand workspace, We first determine the robot thumb abduction joint by make it equal the human thumb abduction joint  $T_0$ . Then using the method similar to [5], we check the workspace boundaries of the robot hand and find the closest one to the desire position, where the approximate pose can be generated by the inverse kinematics.

## V. SIMULATION SYSTEM AND TELEOPERATION EXPERIMENTS

### A. Simulation System

We developed a 3D graphics simulation system using the OpenInventor® to visualize and test the modified mapping method in a SGI workstation. As shown in Fig. 6, in the right, human hand model is manipulated by the operator with a CyberGlove®; in the left, the dexterous robot hand model follows the motion generated by the modified fingertip mapping method.

In the 3D graphics system, a layered oriented tight-fitting bounding box tree has been established to approximate to each geometrical model of fingers and objects for grasping. Taking advantage of the theorem of separated axis [10], real-time accurate and fast collision detection among moving geometrical models can be achieved. Using the method of searching the nearest feature pair of the geometrical models [11], it can achieve the model distances between the moving fingers and the objects. If fingers and the object contact, a contact warning message will show to the operator.

The simulation system was developed to bridge a gap between teleoperation experiments and software development

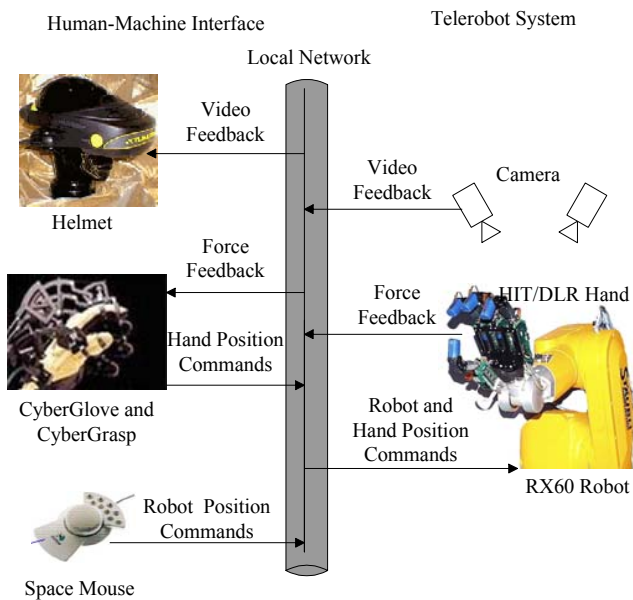


Fig.7 teleoperation system structure with vision and force feedback

activities. In the simulation system, we can validate the modified fingertip mapping without directly controlling with the HIT/DLR hand, which assures that no damage to the robot hand. In the simulation process, the 3D graphics testing shows that the human model is precise enough to describe the human hand motion and the mapping method can continuously calculate the approximate pose on real time when the fingertip position is out of the workspace of the robot hand.

### B. Teleoperation Experiments

We have developed a robot hand/arm teleoperation system in our local area network, where the operator sends robot hand/arm position commands and receives visual and force feedback information, as shown in Fig. 7.

In the teleoperation system, we use the space mouse as the 3D input device, which has six DOFs and can control the end point position and pose of the Staubli RX60 robot. We map the human hand motion to control the dexterous robot hand: when performing power grasps, the system adopts the joint space mapping method that motions of human hand joints are directly transferred to the robot hand and the operator can adjust the posture interactively; when performing the precise tasks, the system adopts the modified fingertip position mapping method.

Force sensors are built into HIT/DLR hand. CyberGrasp<sup>TM</sup> exo-skeleton can create one dimensional force feedback per finger. The forces imparted on the fingers can be displayed to the operator by means of CyberGrasp<sup>TM</sup>. Visual feedback is provided by a stereo display helmet and includes live video from two whole scene cameras. The visual feedback provides a view into the robot's environment, facilitating intuitive operation and natural interaction with the work site.

Some tasks were performed to evaluate the mapping method. We have performed the task that pouring water from a bottle with the power grasp, which can test the joint space

mapping method. Also, we performed some teleoperation tasks to test modified fingertip position mapping method such as: grasping a litter cube block only with index finger and thumb; grasping a bulb and a table tennis ball with four fingers.

## VI. CONCLUSION AND FUTURE WORK

An interface that enables people to control the HIT/DLR dexterous hand with the CyberGlove<sup>®</sup> has been developed. The parameters of the human hand model are calibrated by the open-loop calibration method based a vision system. The joint space mapping and modified fingertip position mapping method are exercised in the manipulation of dexterous robot hand. Teleoperation experiments show that the human hand model is sufficient accuracy for teleoperation task. The mapping system allows the operator to easily and intuitively manipulate the objects.

In our next research, we will continuously improve the system integration, accuracy and dexterity. Next step, we want to integrate the vision, force sensors and make the robot arm/dexterous hand system perform some manipulation autonomously.

## REFERENCES

- [1] Rohling, R., and Hollerbach, J.M., " Modeling and parameter estimation of the human index finger," Proc. IEEE Intl. Conf. Robotics and Automation, San Diego, May 8-13, 1994, pp. 223-230.
- [2] Fischer, M, van der Smagt, P., Hirzinger, G., 1998, "Learning techniques in a dataglove based telemanipulation system for the DLR Hand," 1998 IEEE ICRA, pp1603-1608.
- [3] W.B. Griffin, R.P. Findley, M.L. Turner, and M.R. Cutkosky, "Calibration and mapping of a human hand for dexterous telemanipulation", ASME IMECE 2000 Symposium on Haptic Interfaces for Virtual Environments and Teleoperator Systems.
- [4] Wright, AK, Stanasic, MM, 1990, "Kinematic mapping between the EXOS handmaster Exoskeleton and the Utah/ MIT Dextrous hand", 1990 IEEE Int'l Conf. on Systems Engineering, pp. 809-811
- [5] R.N. Rohling and J.M Hollerbach. "Optimized fingertip mapping for teleoperation of dextrous robot hands". In Proc. IEEE Intl. Conf. Robotics and Automation, pages 3:769--775, Atlanta, May 1993
- [6] X.H. Gau, M.H. Jin, L. Jiang, Z.W. Xie, P. He, L. Yang, Y.W. Liu, R. Wei, H.G. Cai, H. Liu, J. Butterfass, M. Grebenstein, N. Seitz, and G. Hirzinger, "The HIT/DLR Dexterous Hand: Work in Progress," 2003 IEEE ICRA, pp 3164-3169.
- [7] "CyberGlove<sup>®</sup> reference manual", Virtual Technologies Inc., 2000.
- [8] D.E. Whitney, "The mathematics of coordinated control of prosthetic arms and manipulators," ASME J. Dynamic Systems, Meas., Control, pp. 303-309, 1972.
- [9] Schroer, K. 1993. "Theory of kinematic modelling and numerical procedures for robot calibration". Robot Calibration., ed. R.Bernhardt and S.L.Albright. London: Chapman & Hall, 157-196.
- [10] S. Gottschalk, M. C. Lin, D. Manocha. OBBTree: A Hierarchical Structure for Rapid Interference Detection. Proc of SIGGRAPH'96[C]. 1996: 171~180
- [11] Stephen A. Ehmann, Ming C. Lin. Accelerated Proximity Queries Between Convex Polyhedra By Multi-Level Voronoi Marching. Tech. Report TR00-026, Department of Computer Science, Univ. of North Carolina. 2000. 3, 5